Rechargeable lithium battery employing a new ambient temperature hybrid polymer electrolyte based on PVK + PVdF–HFP (copolymer)

M.S. Michael, S.R.S. Prabaharan[*]

Center for Smart Systems and Innovation, Advanced Power Sources Laboratory, Faculty of Engineering
Multimedia University, 63100 Cyberjaya, Malaysia

Abstract

We describe here for the first time, our recent success in developing an ambient temperature Li^+ conducting solid polymer electrolyte (SPE) using the concept of polymer alloying upon blending two thermoplastic polymers such as poly(vinylidene) fluoride-hexafluoropropylene (PVdF–HFP-copolymer) and poly(N-vinylcarbazole), PVK and achieved the room temperature electrolytic conductivity (σ_i) of 0.7×10^{-3} S/cm for a typical composition of PVdF–HFP copolymer/PVK blend mixed with $EC/LiBF_4$ molar composition. The ionic transference number of 0.49 was deduced from combined ac-impedance and dc polarization method. High-resolution optical microscopic examination revealed the disappearance of characteristic highly porous surface structure of PVdF–HFP matrix upon blending with PVK leading to the formation of resultant PVdF–HFP/PVK blend polymer alloy. The electrochemical stability of the polymer electrolyte membrane thus obtained was found to be stable up to ~4.7 V versus Li/Li^+. The new hybrid alloy polymer electrolyte membrane was found to exhibit good interfacial properties against lithium metal and thus, it was found to aid the room temperature operation as electrolytic membrane cum separator in all-solid state rechargeable lithium polymer test cell, $LiCo_{0.8}Ni_{0.2}O_2/SPE/Li$.
© 2004 Elsevier B.V. All rights reserved.

Keywords: Polymer alloy; Poly(N-vinylcarbazole); PVdF–HFP copolymer; Polymer electrolyte; Transference number; Lithium batteries

1. Introduction

Among the critical needs in advanced lithium batteries, lithium polymer battery is a viable solution. Advanced solid polymer electrolytes (SPEs) occupy a place of pride in the new generation lithium secondary battery technology. Today's commercial lithium polymer technology is based on gel type polymer membranes in which ion is immobilized in a solid polymer network, exhibiting semi-solid properties. A large number of studies have been carried out on rechargeable lithium polymer batteries using gel polymer electrolytes in which electrolyte solution has been immobilized by incorporation into a matrix polymer, such as poly(acrylonitrile) (PAN), poly(methylmethacrylate) (PMMA), poly(ethyleneoxide) (PEO) and poly(vinylidene fluoride) (PVdF), etc. While these gel polymer electrolytes exhibit high ionic conductivity exceeding 10^{-3} S/cm, most of them have various deficiencies preventing them from being used in commercial lithium batteries. Substantial research activities have been carried out for the past few

decades to develop polymer electrolytes with all required qualities [1–5].

At the outcome, promising results have been obtained with 'hybrid polymer electrolytes'—a concept of trapping liquid solutions into the polymer cages either carried out by the gellification of polymer with organic electrolyte [6–8] or by injecting organic electrolyte into polymer matrix [9–12]. On the other hand, the ionic conductivity of dry polymer electrolyte prepared simply by the addition of lithium salt is very low, of the order of 10^{-5} S/cm, which is too low to be employed in batteries [13]. However, the addition of plasticizer, namely, gellification might help to improve the ionic conductivity two orders higher (10^{-3} S/cm) but the higher percentage of plasticizer results in poor mechanical strength. To retain the mechanical strength of the polymer, addition of either inert inorganic fillers or another polymer along with the plasticizer has been the viable proposition [14–17]. Generally, blending of two polymers not only results in improving the mechanical strength but also helps increasing the conductivity by suppressing the crystallization of polymer chain in any one of the following ways: (1) cross-linking, (2) copolymerization, (3) comb formation and (4) polymer alloying [18–20]. The latter method has been gaining much attention in the recent past in the context of

* Corresponding author. Tel.: +60-3-83125378; fax: +60-3-83183029.
E-mail address: prabaharan@mmu.edu.my (S.R.S. Prabaharan).

developing solid polymer electrolytes for lithium battery application. It was reported that the addition of inorganic inert fillers has improved the stability of lithium/polymer interface by scavenging water or other liquid impurities [21].

PVdF and its copolymer with hexafluoropropylene (HFP), PVdF–HFP, are of considerable practical interest in view of mass production as well as their high electrochemical properties. The latter can be called as poly(vinylidene fluoride-co-hexafluoropropylene). PVdF–HFP copolymers differ from the pure homopolymer in that a comonomer, hexafluoropropylene, is added to modify the host PVdF structure as shown below:

$$-\{CH_2 - CF_2 -\}_n -\{CF_2 - \underset{\underset{CF_3}{|}}{CF} -\}-$$
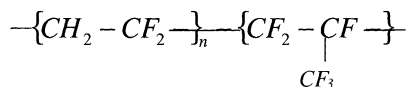
The unique polymer structure of carbon, hydrogen, and fluorine atoms found in polyvinylidene fluoride resins produces polymers that have extremely high thermal and chemical stability and yet retain their thermoplastic nature allowing ease of processing for fabrication.

Recently, ionic conductivity closer to that of non-aqueous electrolyte has been achieved by injection of the liquid electrolyte into the polymer matrix prepared from copolymer, poly(vinylidene) fluoride-hexafluoropropylene (PVdF–HFP) [22]. The porous nature of solid polymeric membrane of PVdF–HFP has an advantage of trapping large quantity (more than 200%) of non-aqueous electrolyte inside its polymer network. Telcordia Technologies Inc. (formerly Bellcore) pioneered the latter approach and the technology was named as PLion^{TM} Technology [12,15] employing PVdF–HFP copolymers as separator cum electrolyte. The presence of HFP comonomers (Dyneon^{TM}) make PVdF more soluble in ethylene carbonate (EC) based liquid electrolyte solutions when the cell temperature is raised to over 60 °C by abusive cell operation [18]. That is, when the temperature of the battery rises abnormally due to overcharge the cell could be shut off due to the low "shut-down" temperature of PVdF. These properties are ideal for battery designs vulnerable to overheating.

In the present study, we produced a different version of Li^+-conducting polymer electrolyte, which is composed of PVdF–HFP copolymer/poly(N-vinylcarbazole) (PVK) blend hybrid polymer electrolyte formed by means of alloying between the above two polymers and studied the effect of micro-structural change of blend membranes, and also examined the electrolytic conductivity (σ_i) and electrochemical properties. Finally, Li-polymer battery performance using the new polymer blend electrolyte, was assembled Li/[PVdF–HFP/PVK+Li^+]/LiCo$_{0.8}$Ni$_{0.2}$O$_2$ and tested at ambient conditions.

2. Experimental

Both polymers, PVdF–HFP copolymer (KYNAR2821 (Elf Atochem Co., France) and PVK (average weight

1,100,000, Aldrich, USA) were vacuum dried at 90 °C over night prior to use. The appropriate quantities of PVdF–HFP:PVK were dissolved in THF (Merck Battery grade) in the following weight ratio, 95:5 and 90:10, and subsequently, stirred for 3 h at 50 °C to obtain homogenous mixture solution. An appropriate molar concentration of LiBF$_4$ (Merck) in EC (battery grade, Merck) was added to the above mixture so as to obtain, *polymer blend:electrolyte*, 80:20 (w/v) composition. The resultant mixture was stirred for 1 h to complete the homogenization of the mixture solution. LiBF$_4$ was preheated over night at 100 °C under vacuum prior to use. Finally, the blend was poured on to a glass plate, covered with another glass plate with holes to facilitate slow evaporation of the solvent. Freestanding dry films were readily obtained upon evaporating the solvent (THF). The films thus obtained were opaque and were heated at 60 °C for 2 h under vacuum to ensure complete evaporation of excess THF. All experiments were carried out inside the argon filled glove box. After complete evaporation of the solvent, the thickness of the polymer film was measured to be within 80–100 μm. For comparison, polymer films with PVdF–HFP(copolymer host) and PVK were prepared separately. The microscopic morphology of polymer films with and without the addition of PVK was studied under a high-resolution optical microscopy by using Metallurgical Microscope, Eclipse ME600L (Nikon) equipped with digital camera at 500× magnification.

Ionic conductivity (σ_i) of the polymer films was deduced by complex ac impedance spectroscopy. The impedance spectra were obtained over a 100 kHz–10 mHz using a PAR Basic Electrochemical System (Perkin-Elmer, USA) equipped with Power Suite software (PowerCV and Powersine). A constant dc bias of 0 V and an ac perturbation voltage of 10 mV (r.m.s.) were applied. The polymer electrolyte membrane sample was contained in a hollow Teflon cell of known dimensions and sandwiched between two SS blocking electrodes in an airtight cell. A typical circular disk sample was 2.0 cm^2 area and 0.09 mm thick (cell constant was measured to be 4.5×10^{-3} cm^{-1}). The temperature-dependent measurements were performed over a temperature range of 298–348 K in a homemade housing where the temperature was regulated within ±0.1 °C.

The electrochemical stability window of the films was measured by linear sweep voltammetry, using a Perkin-Elmer Basic Electrochemical System (PAR, USA). Li metal (FMC Co., USA) was used as counter and reference electrode, and stainless steel (SS) disk (3.14 cm^2) was used as working electrode. Impedance spectra of symmetrical Li/SPE/Li cells were measured under open circuit potential (OCP) condition with time at room temperature.

The Li^+ transference number (t_{Li^+}) of polymeric membrane was measured by the method described by Bruce and Vincent [23]. It consists of measuring the interfacial resistance of a symmetrical cell, Li/SPE sample/Li by means of ac impedance technique and the current across the same cell was measured by chronoamperometry by applying a

constant dc bias. The measurements were taken at the initial time of the applied dc potential ($t = t_0$, $R = R_0$, $I = I_0$) and under steady conditions ($t = t_s$, $R = R_s$, $I = I_s$). By using these values, the t_{Li}^+ was calculated by using the following expression:

$$t_{Li}^+ = \frac{I_s(V - I_0 R_0)}{I_0(V - I_s R_s)} \qquad (1)$$

The Li polymer cells were assembled by sandwiching the dry polymer electrolyte membrane between the composite cathode LT-LiCo$_{0.8}$Ni$_{0.2}$O$_2$ (prepared by a low temperature (LT) solution technique using citric acid as a complexing agent) and lithium metal anode in a spring loaded Teflon^{TM} cell (designed in-house) having 2450 coin cell configuration. Composite cathode was prepared by spreading a mixture of active-electrode material, LT-LiCo$_{0.8}$Ni$_{0.2}$O$_2$, 75%, conductive carbon 5% (KS6) and PVdF–HFP/PVK polymer electrolyte slurry, 20% onto a special Al mesh (Exmet, USA). Thickness of the cathode film was controlled within ∼200 μm using a doctor blade. The galvanostatic charge/discharge performance was carried out between 2.7 and 4.4 V (Arbin multichannel Battery testing system, BT2000, Arbin Instruments, USA).

3. Results and discussion

Poly(*N*-vinylcarbazole) is a carbazole derivative of polyvinyl chloride (PVC) in which a chlorine atom has been substituted by carbazole group and its chemical formula is as below
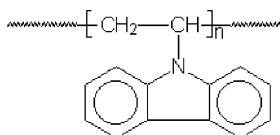
Here, we have used PVK as a blending agent to modify the host PVdF–HFP copolymer matrix while the former still provides the plasticizer action. The X-ray diffractograms recorded for PVdF–HFP/PVK did not show any noticeable changes with respect to pure PVdF–HFP and both diffractograms exhibit disordered structure indicative of the glassy nature of amorphous polymer matrix. This indicates that the
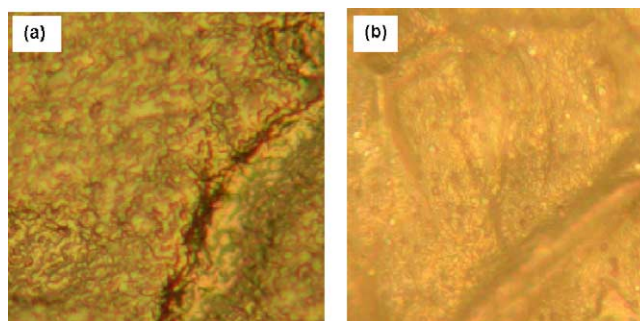

Fig. 1. Optical microscopic images (500×) of polymer electrolytes showing the surface texture. (a) Pure PVdF–HFP electrolyte; (b) PVdF–HFP/PVK blend electrolyte.

incorporation of PVK into PVdF–HFP copolymer matrix retains its glassy nature as evidenced by XRD examination (not shown here). Fig. 1a and b shows the high-resolution optical micrographs of polymer electrolyte corresponding to pure PVdF–HFP copolymer prepared with LiBF$_4$/EC (sample 1) and PVdF–HFP/PVK mixed with LiBF$_4$/EC (sample 6), respectively. The highly porous nature of the PVdF–HFP copolymer as shown in Fig. 1a was disappeared upon blending with PVK (Fig. 1b) indicative of the mutual compatibility of the two polymers with one another. Also, XRD patterns also reveal the possibility of alloying reaction between the two polymers due to their favorable free energy of interaction.

The ionic conductivity of a polymer film prepared from PVdF–HFP (host) by conventional gellification technique with 1.5 M LiBF$_4$/EC renders the ionic conductivity of 0.16×10^{-3} S/cm at room temperature but mechanical strength of the polymer film was obviously poor. However, the addition of PVK was found to enhance its conductivity ∼4.5 times higher (0.72×10^{-3} S/cm) than that of the above composition without PVK. In addition, interaction with PVK phase enhances its mechanical strength, while the thermoplastic stability is an additional feature of the polymeric membrane developed in the present work. The compositions of different polymeric membranes studied in the present work together with their room temperature ionic conductivity are summarized in Table 1.

For an optimized composition corresponding to sample 6 as shown in Table 1, the highest ionic conductivity of

Table 1
Compositional dependence of ionic conductivity (σ_i)

Sample no.	Composition (%)	Ionic conductivity, σ_i (mS/cm) at 298 K
1[a]	PVdF–HFP 28%, EC 62%, LiBF$_4$ 10%	0.157
2	PVdF–HFP 28%, EC 62%, LiBF$_4$ 10%	0.298
3	PVdF–HFP 26.6%, PVK 1.4%, EC 65%, LiBF$_4$ 7%	0.459
4	PVdF–HFP 252%, PVK 2.8%, EC 65%, LiBF$_4$ 7%	0.579
5	PVdF–HFP 26.6%, PVK 1.4%, EC 62%, LiBF$_4$ 10%	0.531
6[b]	PVdF–HFP 25.2%, PVK 2.8%, EC 62%, LiBF$_4$ 10%	0.713
7[c]	PVK 28%, EC 62%, LiBF$_4$ 10%	0.062

[a] Composition without PVK.
[b] Composition corresponding to maximum electrolytic conductivity (σ_i) at 298 K.
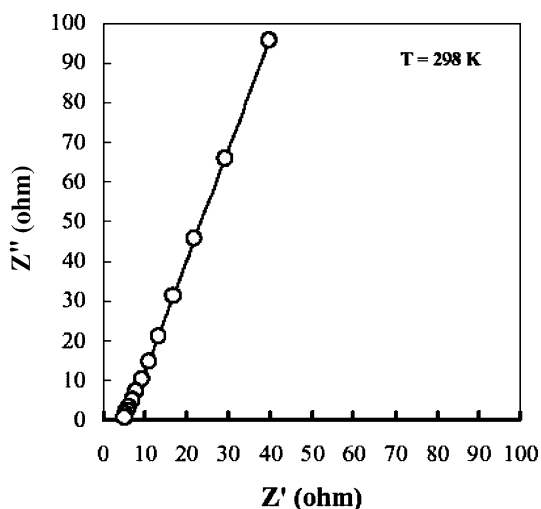[c] Composition without PVdF–HFP.

Fig. 2. The impedance plot for a PVdF–HFP/PVK blend electrolyte (PVdF–HFP 25.2%, PVK 2.8%, EC 62%, LiBF$_4$ 10%: sample 6) at room temperature (cell constant $= 4.5 \times 10^{-3}$ cm^{-1}).

0.72 mS/cm was deduced at room temperature. The Nyquist plot of sample 6 (Table 1) is shown Fig. 2. As shown in Fig. 2, the impedance response is quite linear exhibiting a spike (tail-like character) indicative of the characteristic electrolytic behavior of the polymeric membrane in its dry state. Also, it exemplifies the good physical integrity and homogeneous nature of the membrane otherwise semicircle appears in high frequency due to lack of homogeneity resulting from crystallization, liquid loss and/or phase separation.

Polymeric membrane of dry and free-standing type, possessing good mechanical stability was obtained upon addition of 5–10% of PVK into PVdF–HFP copolymeric host and upon further increasing the concentration of PVK was resulted in poor film formation. The increase in ionic conductivity by the addition of PVK might be attributed to the plasticizer action into the host (PVdF–HFP).

The blending of PVK into host PVdF–HFP copolymer matrix likely to suppress the crystallization of polymer chain due to the formation a polymer alloy and thus improvises the polymer chain mobility that resembles similar to the first generation category of SPE. Recently, Abraham et al., reported that the addition of poly(ethyleneglycol), PEG oligomer as a plasticizer into the PVdF–HFP copolymer-based polymer electrolyte and they have called this system namely "PEO-like" polymer electrolyte [24]. The percentage addition of PVK into host PVdF–HFP copolymer matrix with respect to room temperature ionic conductivity was optimized and monitored the mechanical stability together with dry appearance of the freestanding film. The effect of increasing the concentration of lithium salt, LiBF$_4$ in the polymer electrolyte with respect to ionic conductivity was also studied in order to obtain the well-balanced polymer/electrolyte composition. As expected, changing the concentration of electrolyte solution from 1.5 to 2.0 M LiBF$_4$ in EC has increased the
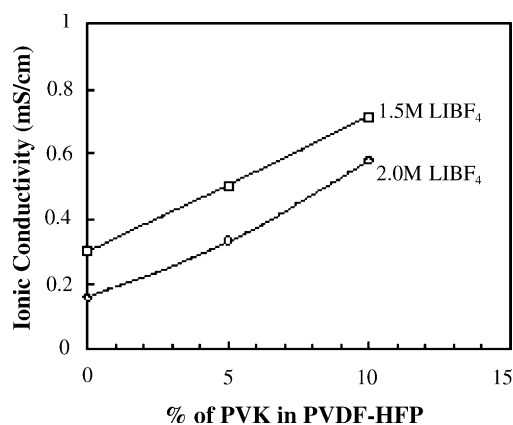

Fig. 3. Variation of ionic conductivities at room temperature with respect to two different molar concentration of LiBF$_4$/EC liquid electrolyte.

ionic conductivity significantly (Fig. 3). We also studied the ionic conductivity of the polymer film prepared using PVK as the polymer host mixed with EC/LiBF$_4$ and found to be 6.2×10^{-5} S/cm at room temperature.

Impedance measurements were obtained along a temperature ramp to determine the temperature-dependent conductivity of the best conducting composition (sample 6 in Table 1) of the blend electrolyte sample. The data were then plotted on Arrhenius coordinates as shown in Fig. 4. The bulk resistance (R_b) was determined from high frequency intercept on the real axis in complex impedance, then σ is calculated by the equation $\sigma = l/AR_b$, where A is the area and l is the thickness of membrane. A typical Vogel–Tamman–Fulcher (VTF) conductivity–temperature relationship was observed in the temperature range of 30–75 °C from the temperature dependence of ionic conductivity plot (Fig. 4). As seen in Fig. 4, the positive curvature (nonlinearity) indicates that ionic conduction obeys the empirical Vogel–Tamman–Fulcher relationship (Eq. (2)), which describes the transport properties in a viscous matrix [25–27]
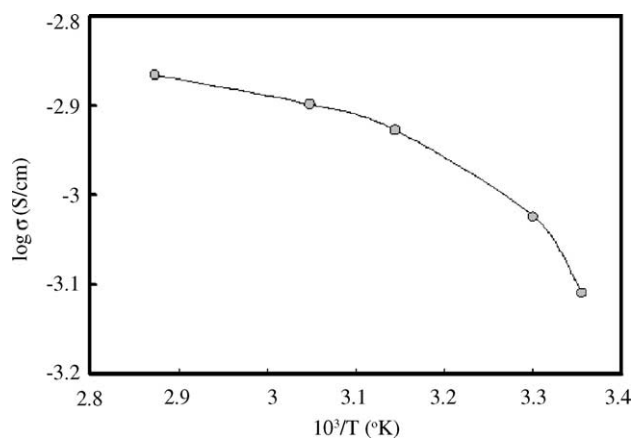

Fig. 4. Arrhenius curve showing the variation of ionic conductivity of PVdF–HFP/PVK blend electrolyte (sample 6) at different temperatures.
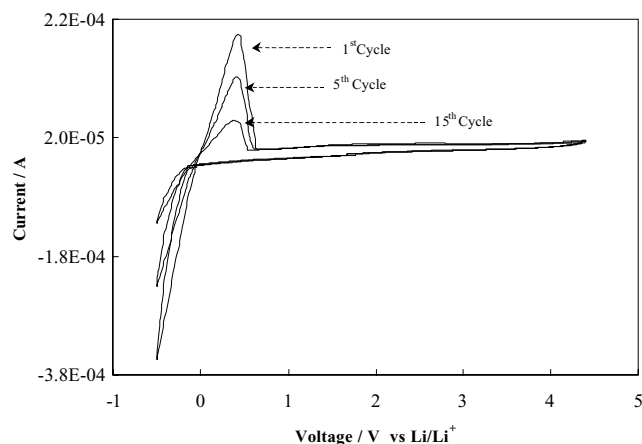
Fig. 5. Cyclic voltammogram of SS/LiBF$_4$–EC–(PVdF–HFP)–PVK/Li; lithium plating/stripping on the SS electrode for the polymer blend electrolyte is shown for the best conducting polymer electrolyte blend (sample 6). Working electrode, SS; counter and reference electrode, lithium; scan rate = 5 mV/s.

$$\sigma(T) = AT^{-1/2} \exp\left[\frac{-B}{k_{B}(T - T_{0})}\right] \qquad (2)$$

where A is a constant proportional to the number of charge carriers, B is the pseudo-activation energy related to polymer segmental motion, k_{B} is the Boltzmann constant, and T_{0} is a reference temperature associated with ideal T_{g}. These relationships imply that the main mechanism of ionic conduction can be explained by free volume theory.

The conductivity (σ_{i}) of pure PVdF–HFP/EC + LiBF$_4$ film (sample 2) was 0.30×10^{-3} S/cm at room temperature (298 K) but that of PVdF–HFP/PVK + EC + LiBF$_4$ film was as high as 0.72×10^{-3} S/cm at ambient temperature. These values are one order less than that of EC/DMC/LiPF$_6$ conventional liquid electrolyte conductivity of 1×10^{-2} S/cm at room temperature. However, the ionic conductivity of PVdF–HFP/PVK + EC + LiBF$_4$ blend electrolyte film reaches a value of 1.36×10^{-3} at 75 °C. Of course, this value is roughly three times less than those of PVdF–HFP gel film electrolyte ca. 4×10^{-3} S/cm [28].

Fig. 5 shows typical cyclic voltammogram (CV) of Li/sample 6/SS cell at a scan rate of 5 mV/s between −0.5 and 4.4 V. CV exhibits two peaks corresponding to lithium deposition onto stainless steel at −0.49 V and stripping of lithium at 0.43 V during the reverse scans. No other additional peaks were observed indicating the absence of any electro-active impurities in the film such as residual water, etc. To find out the oxidation (electrolyte decomposition) potential of the polymer electrolyte, a linear sweep voltammetry of the cell, Li/sample 6/SS was carried out above 4 V at a sweep rate of 0.1 mV/s and it is depicted in Fig. 6. Linear sweep voltammetry is generally used to study the electrochemical stability window of a given polymer electrolyte using the Li/SPE/SS cell configuration. The onset of the current in the anodic high voltage range is assumed to result from a decomposition process associated with elec-
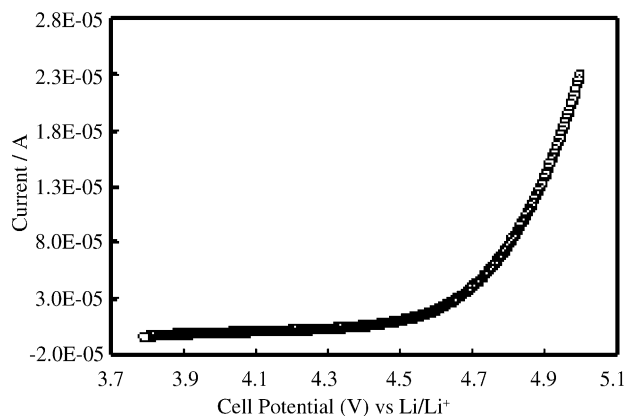

Fig. 6. Linear sweep voltammetry (scan rate: 0.1 mV/s) curve (current–voltage curve) of SS/LiBF$_4$–EC–(PVdF–HFP)–PVK/Li cell at room temperature (25 °C). The onset of the current occurs at the decomposition voltage of the electrolyte.

trode/electrolyte [29] and this onset voltage is taken as the upper limit of the electrolyte stability range. This voltage is generally located as the point of intersection of the extrapolated linear current in the high voltage region with the voltage axis. For all blend electrolytes studied, the current responses were negligible below 4.5 V versus Li/Li$^+$. This implies that there is no decomposition of any components in this potential region and PVdF–HFP/PVK blend electrolytes have suitable electrochemical stability for highly oxidizing cathode materials such as LiCoO$_2$, LiNiO$_2$ and LiMn$_2$O$_4$. It is evident that the onset of current in the anodic high voltage probably due to the decomposition of the electrolyte possibly occurs at ∼4.7 V that coincides with the oxidation of lithium salt LiBF$_4$. It seems that the addition of PVdF–HFP and PVK did not affect the decomposition potential of the lithium salt LiBF$_4$. Work is in progress to examine the above polymeric membrane with other lithium salts/solvent composition in the context of improving the electrochemical stability window.

Impedance analysis was used to study the interfacial phenomena of nonblocking Li/SPE/Li cells. Fig. 7 shows a typical impedance spectrum of Li metal/SPE interface under OCP condition with time at room temperature. The interception at high frequency can be assigned to electrolyte resistance (R_{e}), and the intercept on the low frequency side corresponds to interfacial resistance (R_{i}). It is found that the R_{e} value of PVdF–HFP/PVK + EC + LiBF$_4$ blend electrolyte was almost constant at room temperature within 144 h (the maximum elapsed time studied in the present work). In the case of interfacial resistance, the progressive expansion of R_{i} indicates the continuous growth of a passivation layer on the Li metal surface [30]. This resistive layer is known to occur as a result of the reaction between aprotic solvent (EC) and Li metal electrode.

The compatibility of the polymer electrolyte with electrodes was examined by electrochemical impedance spectroscopy (EIS) as this is an effective tool to characterize the formation of passivation layer on both sides of the
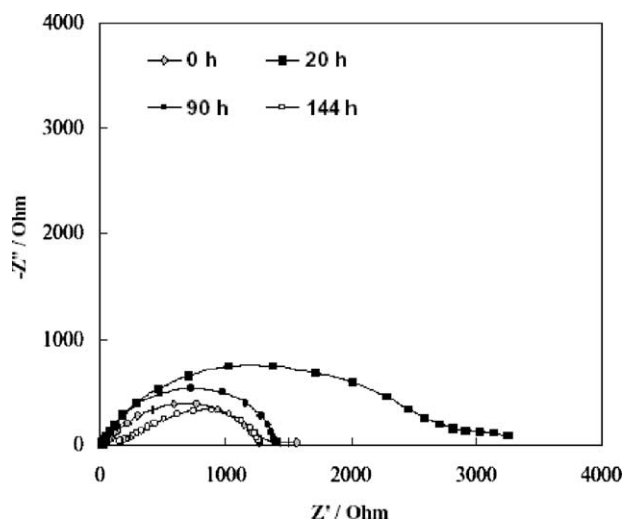
Fig. 7. Time evolution of the Impedance spectra of the nonblocking Li/LiBF$_4$–EC–(PVdF–HFP)–PVK/Li cell showing the Li metal/SPE interface under open circuit potential (OCP) condition with time at room temperature (25 °C).

Fig. 9. The ac impedance spectra of a Li/LiBF$_4$–EC–(PVdF–HFP)–PVK/Li symmetric cell at room temperature (25 °C) before ($t = 0$ h) and after polarization ($t = 4$ h) with total applied potential difference of 20 mV.

electrodes and its interfacial reaction during cell cycling in situ. This information would be useful to understand the stability of the passivation layer upon repeated cycling which could help determine the irreversible loss during the first cycle and the reversible capacity of cell during subsequent cycles.

The time evolution impedance spectra of Li/sample 6/LiCo$_{0.8}$Ni$_{0.2}$O$_2$ cell as a whole kept under the open circuit condition at room temperature (not shown). It is noted that the semicircle at medium-high frequency might be associated with charge transfer resistance and resistance of poorly conducting surface film on the electrode increases initially and then tends to stabilize as the cell approaches equilibrium. At the same time, the potential of the cell decreased from 3.5 V (measured as soon as fabricated) to 3.2 V in 2 h of equilibrium confirming the formation of passivation film. This result is in good agreement with earlier result that
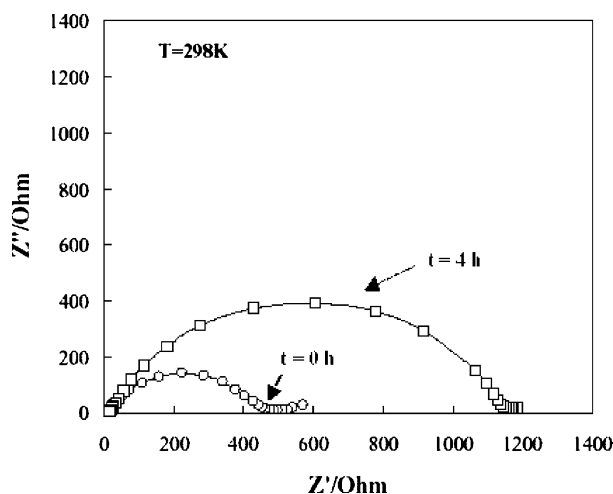
passivation layer has been formed on the surface transition metal oxides similar to carbonaceous anode in non-aqueous aprotic electrolytes [31]. In the present case, the main cause for the passivation film formation on the electrode surface is attributed to the presence of ethylene carbonate in the polymer electrolyte.

As the cell is being cycled, the shape and magnitude of medium-high frequency semicircle arc has been changed with respect to deintercalated lithium. In a real case, the passivation film on the surface of transition metal oxide has been taken into account, the deintercalated lithium from the cathode has to undergo different processes before reaching the lithium anode. That is, as a first step, it has been deintercalated by solid-state diffusion from the cathode accompanied by interparticle electron transfer. Then it reaches cathode/passivation film interface where charge transfer takes place subsequently it migrates through the poorly conducting passivation layer. Finally it reaches
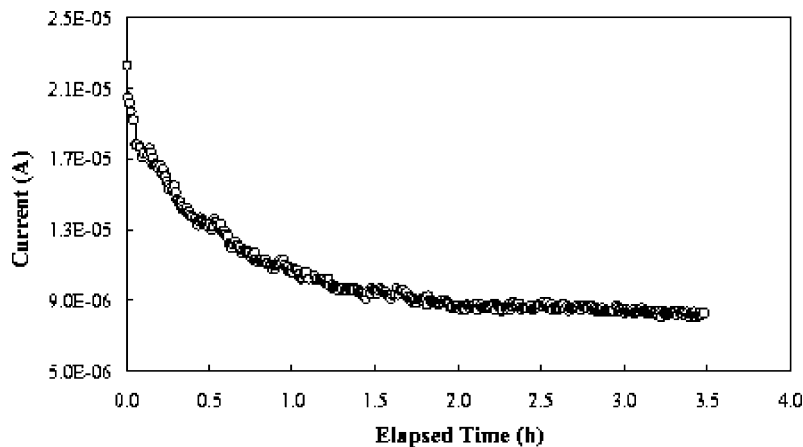

Fig. 8. Variation of the current with time during polarization of a Li/LiBF$_4$–EC–(PVdF–HFP)–PVK/Li symmetric cell at room temperature (25 °C), with an applied potential difference of 20 mV.
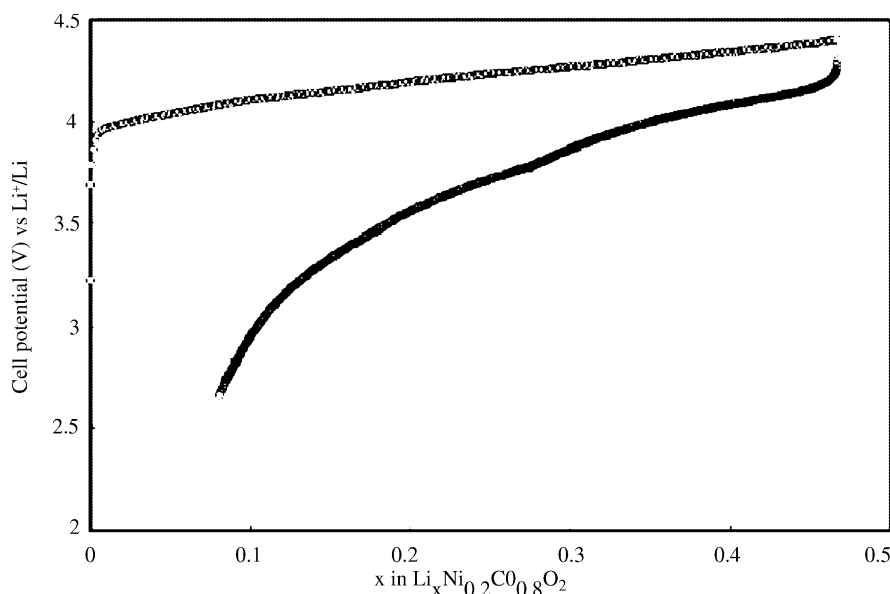
Fig. 10. First charge/discharge cycle of $LiCo_{0.8}Ni_{0.2}O_2/LiBF_4$–EC–(PVdF–HFP)–PVK/Li at a rate of 2 mA/g between 2.7 and 4.4 V at room temperature (25 °C).

the passivation film/polymer film and migrates through the polymer film accompanied by charge transfer. Similarly, at the anode side (Li^0), it once again follows the multi-step processes before being deposited onto lithium anode. Interestingly, the EIS spectra of the cathode consist of semicircle at high-medium frequency (supposed to be non-potential dependant) followed by another semicircle (potential dependant) due to charge transfer at different interfaces and ends with Warburg line due to diffusion. Sometimes, the two semicircles merged together and hence the amplitude of semicircle changes with cell potential. Interestingly, in our case, we observed a single semicircle (not shown) that changed with the amount of lithium extracted, in other words changes with cell potential. The semicircular arc is bigger for 0.1 Li and starts to become smaller as the amount of lithium extracted was increased. It could be explained by passivation film formation, which might be stopped when the amount of extracted lithium reaches a value of 0.1 M per formula unit of the cathode material.

The knowledge of ion transference number (Li^+) in the polymer electrolyte is an important aspect as the transport of lithium ions during intercalation plays a vital role on the performance of the polymer batteries. It is understood that polarization due to concentration gradient in the cell is minimized if the fraction of current carried by lithium ion, i.e., transference number approaches one. Therefore, to measure the ion transference number, the interfacial resistance of the cell, Li/sample 6/Li has been measured before and after the polarization of cell by applying a small voltage pulse of 20 mV. During polarization the current passed through the cell has been measured and found that it has reached steady-state value after 4 h as shown in Fig. 8.

Fig. 9 shows the impedance responses of the above cell measured before and after the polarization in order to extract the change in interfacial resistance. Based on the measured parameters and upon using Eq. (1), the transference number has been calculated to be 0.49 for sample 6. A test cell employing presently developed SPE, Li/sample 6/$LiCo_{0.8}Ni_{0.2}O_2$, has been subjected to constant current charge and discharge cycle at the rate of 2 and 1 mA/g, respectively and its typical first charge/discharge graph is shown in Fig. 10. As seen from Fig. 10 that the hysteresis observed between the charge and discharge curve and irreversible loss in the first cycle may be due to over voltage resulted from the formation of passivation film on the cathode. The low polarization voltage between charge and discharge is noteworthy. More work is in progress to study the cycle life stability of this new polymer electrolyte and the effect of other lithium salts in the presence carbonate aprotic solvents are currently under progress and will be published elsewhere.

4. Conclusion

We have demonstrated for the first time that [PVdF–HFP–PVK] + [EC/$LiBF_4$] blend polymer electrolyte film provides the room temperature electrolytic conductivity of 0.72 mS/cm with an ionic transference number of 0.49. The role of addition of PVK to the copolymer matrix, PVdF–HFP was discussed in the light of polymer alloying by means of blending of the above two miscible polymers. Various electrochemical analyses confirm the electrolytic nature of the above polymer electrolyte system developed in the present work which depicts the PEO-like behavior. The

electrochemical stability of the newly developed polymer electrolyte was found to be ~4.7 V. Upon employing the present polymer electrolytic membrane in a rechargeable cell couple, $LiNi_{0.2}Co_{0.8}O_2$/new SPE/Li, the reversible capacity of ~120 mAh/g is achieved which is indeed a reasonable value while employing a polymer electrolyte at room temperature.

Acknowledgements

References

[1] M.B. Armand, J.M. Chabango, M.J. Duclot, Fast Ion Transport on Solids, Elsevier/North-Holland, New York, 1979.
[2] D.E. Fenton, J.M. Parker, P.V. Right, Polymer 14 (1973) 589.
[3] G. Nagasubramanian, S. Distefano, J. Electrochem. Soc. 137 (1990) 3830.
[4] F. Capuano, F. Croce, B. Scrosati, J. Electrochem. Soc. 138 (1991) 1918.
[5] C. Capiglia, Y. Saito, H. Yamamoto, H. Kageyama, P. Mustrrelli, Electrochim. Acta 45 (2000) 1341.
[6] Z. Jiang, B. Carrol, K.M. Abraham, Electrochim. Acta 42 (1997) 2667.
[7] C.S. Kim, S.M. Oh, J. Power Sour. 109 (2002) 98.
[8] G.B. Appetechi, F. Croce, R. Marassi, L. Persi, P. Romagnoli, B. Scrosati, Electrochim. Acta 45 (1999) 23.
[9] T. Michot, A. Nishimoto, M. Watanabe, Electrochim. Acta 45 (2000) 1347.
[10] M.C. Caravanier, B.C. Montigny, D. Lemordant, G. Bosser, J. Power Sour. 107 (2002) 125.
[11] J.Y. Song, Y.Y. Wang, C.C. Wan, J. Electrochem. Soc. 147 (2000) 3219.
[12] J.M. Tarascon, A.S. Gozdz, C.N. Schmutz, F. Shokooki, P.C. Warren, Solid State Ionics 49 (1996) 8;
F. Croce, B. Scrosati, Chem. Mater. 4 (1992) 1134.
[13] F.M. Gray, Solid Polymer Electrolytes, Fundamentals and Technological applications, VCH, New York, 1991.
[14] C. Liquan, in: B.V.R. Chowdari, S. Radhakrishna (Eds.), Materials for Solid State Batteries, World Scientific, Singapore, 1986, p. 69.
[15] A.S. Gozdz, C.N. Schmutz, J.M. Tarascon, P.C. Warren, US Patent 554 0741 (1996).
[16] M. Matsumoto, T. Ichino, S. Nishi, J. Electrochem. Soc. 142 (1995) 3053.
[17] J.E. Weston, B.C. Steele, Solid State Ionics 7 (1982) 7.
[18] K. Murata, S. Izuchi, Y. Yoshihisa, Electrochim. Acta 45 (2000) 1501.
[19] K. Noda, in: Proceedings of the First International Conference on Polymer Batteries and Fuel Cells, South Korea, June 2003.
[20] S.R.S. Prabaharan, M.S. Micahel, in: Proceedings of the First International Conference on Batteries and Fuel Cells, South Korea, June 2003.
[21] M.C. Broghini, M. Mastragostina, S. Passerini, B. Scrosai, J. Electrchem. Soc. 142 (1995) 2118.
[22] F. Croce, S.D. Brown, S. Greenbaum, S.M. Slane, M. Salomon, Chem. Mater. 5 (1993) 1268.
[23] P.G. Bruce, C.A. Vincent, J. Electroanal. Chem. 225 (1987) 1.
[24] K.M. Abraham, Z. Jiang, B. Carroll, Chem. Mater. 9 (1997) 1978;
K.M. Abraham, A. Jiang, J. Electrochem. Soc. 144 (1997) L136.
[25] H. Vogel, Phys. Z. 22 (1922) 645.
[26] V.G. Tamman, H.Z. Hesse, Anorg. Allg. Chem. 19 (1926) 245.
[27] G.H. Fulcher, J. Am. Ceram. Soc. 8 (1925) 339.
[28] M.-Y. Song, Y.-T. Kim, Y.T. Kim, B.W. Cho, B.N. Popov, H.-W. Rhee, J. Electrochem. Soc. 150 (2003) A439.
[29] S. Slane, M. Salomon, J. Power Sour. 55 (1995) 7.
[30] Y. Xia, K. Tatsum, T. Fujieda, P.P. Prosini, T. Sakai, J. Electrochem. Soc. 147 (2000) 2050.
[31] C. Schmutz, J.M. Tarascon, A.S. Gisdz, P.C. Warren, F.K. Shokoohi, in: Proceedings of the Electrochemical Society Meeting, Miami, FL, October 1994 (abstract no. 109).